

# Microstructural and magnetic studies of Mn–Al thin films

P. C. Kuo

*Institute of Materials Science and Engineering, National Taiwan University, Taipei 107, Taiwan*

Y. D. Yao

*Institute of Physics, Academia Sinica, Taipei 115, Taiwan*

J. H. Huang and S. C. Shen

*Institute of Materials Science and Engineering, National Taiwan University, Taipei 107, Taiwan*

J. H. Jou

*Department of Materials Science and Engineering, Tsing Hua University, Hsinchu 300, Taiwan*

Mn–Al thin films with high coercivity and high saturation magnetization were successfully fabricated by rf magnetron sputtering with properly controlled chemical composition, substrate temperature, and annealing temperature. A high coercivity of about 3000 Oe and a saturation magnetization of about 420 emu/cc have been achieved. We have observed that during annealing at 410 °C, the nonmagnetic  $\epsilon$  phase with a grain size of roughly 100 nm transforms into a metastable ferromagnetic  $\tau$  phase with a platelike grain size of roughly 300 nm. From the continuous measurement of the stress of the films in vacuum as a function of temperature, we observed a compression stress during heating below 220 °C, and a tension stress above 220 °C during cooling. The structure phase transformation from  $\epsilon$  to  $\tau$  phases was related to the stress variation from compression to tension. The high coercivity can be explained by the high magnetocrystalline anisotropy constant of the  $\tau$  phase and the magnetoelastic energy arises from the residual stress of Mn–Al films after the shear transformation. © 1997 American Institute of Physics. [S0021-8979(97)21308-3]

## INTRODUCTION

In the bulk Mn–Al alloy system, a wide range of compositions has been studied extensively, and only the alloys containing about 50–60 at. % Mn exhibit a ferromagnetic phase. This ferromagnetic phase has been identified as a metastable  $\tau$  phase that is a tetragonal  $Ll_0$ -type superstructure so that the magnetic moments of Mn atoms in alloys are parallel to each other.<sup>1–5</sup> It is well known that the high-temperature nonmagnetic hexagonal-closed-packed  $\epsilon$  phase transforms into an orthorhombic  $\epsilon'$  phase by an ordering reaction and then to a metastable face-centered tetragonal ferromagnetic  $\tau$  phase by a martensitic mode.

In a filmtypic MnAl alloy system, because the magnetic properties of Mn–Al alloys are processing sensitive, it is quite difficult to obtain pure MnAl  $\tau$ -phase alloy films with high saturation magnetization and high coercivity.<sup>6–10</sup>

## EXPERIMENT

The MnAl alloy films containing Mn between 30 and 70 at. % were prepared by rf magnetron sputtering. The targets were made from a high purity Al (99.999%) disk and overlaid with small high purity Mn (99.99%) pieces. This arrangement provides a wide range of effective target compositions and, therefore, film compositions. Films were deposited on glass substrates at a substrate temperature  $T_s$  range between 30 and 200 °C. The substrate holder was rotated during deposition. The rf power was controlled with a deposition rate of 0.5 nm/s. The base pressure in the chamber was  $5 \times 10^{-7}$  Torr, and after the high purity Ar gas was introduced, the pressure was kept at 1 mTorr. A typical thickness of the films was 0.8  $\mu\text{m}$ . Thermal annealing was carried out at a temperature between 350 and 550 °C in vacuum. The

microstructure of the films was characterized by x-ray diffractometer and transmission electron microscopy diffraction technique and their compositions were determined by an electron probe microanalyzer (EPMA) calibrated by a standard bulk  $\text{Mn}_{55}\text{Al}_{45}$  alloy. A vibrating sample magnetometer was used for the magnetic studies. The stress variation of the film samples during the annealing process was studied by using a bending beam method. Under this method, the film sample was clamped in the vacuum oven, and from the reflection of a He–Ne laser beam, we converted the signal of the deflection position of the laser beam into the stress value continuously.

## RESULTS AND DISCUSSION

The Mn–Al alloy films containing Mn between 30 and 70 at. % were prepared by the rf magnetron sputtering technique. The compositions were determined by the EPMA technique. The relation between the substrate temperature and the magnetic properties of the films has been measured systematically. At first, we noticed that the concentration of the  $\epsilon$  phase in the as-deposited samples varied as the substrate temperature was varied. For example, Fig. 1(a) shows the x-ray diffraction patterns for the as-deposited  $\text{Mn}_{50}\text{Al}_{50}$  films with substrate temperatures (a) 200 °C, (b) 100 °C, and (c) 30 °C. It is clear that the intensity of the  $\epsilon$  phase peaks increased with decreasing substrate temperature and the half-width of the peaks also decreased with decreasing the substrate temperature. This indicates that the films deposited at a lower  $T_s$  have a larger and more perfect crystalline  $\epsilon$ -phase structure than the films deposited at higher  $T_s$ . From the magnetization measurement of all the as-deposited films, the magnetizations of all the as-deposited samples are very low.

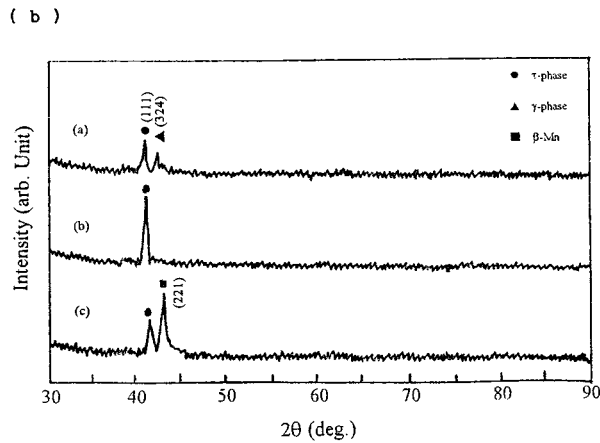
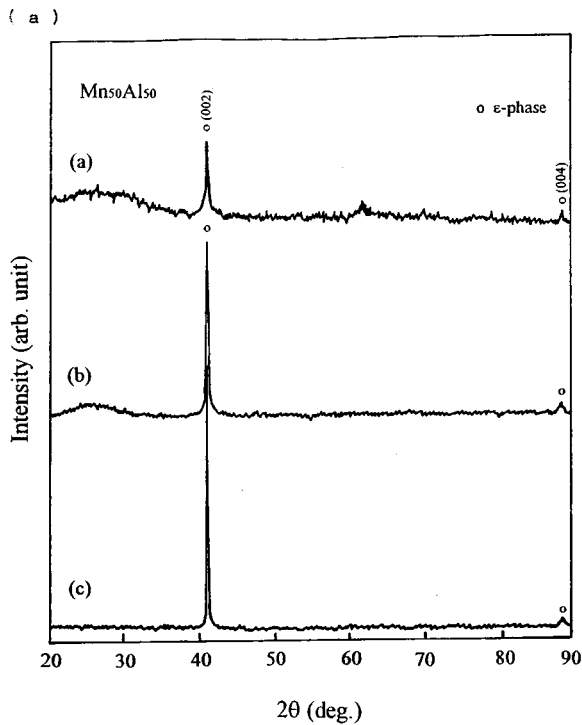


FIG. 1. (a) X-ray diffraction patterns of the as-deposited  $\text{Mn}_{50}\text{Al}_{50}$  films with substrate temperature (a) 200 °C, (b) 100 °C, and (c) 30 °C. (b) X-ray diffraction patterns of the MnAl films with Mn concentration of (a) 44 at. %, (b) 50 at. %, and (c) 56 at. %, after annealing at 410 °C for 30 min.

After annealing at temperatures between 350 and 550 °C in vacuum for 30 min, only the sample with  $\text{Mn}_{50}\text{Al}_{50}$  showed the highest saturation magnetization, the highest coercivity, and almost pure  $\tau$  phase. For explanation, Fig. 1(b) shows the x-ray diffraction patterns of three MnAl film samples with Mn concentrations of (a) 44, (b) 50, and (c) 56 at % after annealing at 410 °C for 30 min. Only the  $\text{Mn}_{50}\text{Al}_{50}$  sample shows an almost pure  $\tau$ -phase diffraction peak. There are always coexisting other phases for all samples besides  $\text{Mn}_{50}\text{Al}_{50}$ . For example,  $\gamma$  phase in  $\text{Mn}_{44}\text{Al}_{56}$ , and  $\beta$ -Mn in  $\text{Mn}_{56}\text{Al}_{44}$  as shown in Fig. 1(b).

From the magnetic measurements of the samples after annealing between 350 and 550 °C, we found that the best condition was annealing at 410 °C for 30 min and the ferromagnetic phase appeared at a composition range between 40 and 60 at. % Mn. Table I lists the saturation magnetization

TABLE I. Magnetic properties of various MnAl film samples after annealing at 410 °C for 30 min.

Film composition	$M_s$ (emu/cc)		$H_c$ (Oe)	
	$T_s=30$ °C	$T_s=100$ °C	$T_s=30$ °C	$T_s=100$ °C
$\text{Mn}_{30}\text{Al}_{70}$	0	0	0	0
$\text{Mn}_{35}\text{Al}_{65}$	10	5	20	15
$\text{Mn}_{40}\text{Al}_{60}$	30	20	150	130
$\text{Mn}_{43}\text{Al}_{57}$	140	40	1580	700
$\text{Mn}_{48}\text{Al}_{52}$	340	90	2400	1300
$\text{Mn}_{50}\text{Al}_{50}$	420	220	3000	1750
$\text{Mn}_{54}\text{Al}_{46}$	270	80	1650	1100
$\text{Mn}_{60}\text{Al}_{40}$	25	30	200	170
$\text{Mn}_{64}\text{Al}_{36}$	15	10	50	35
$\text{Mn}_{70}\text{Al}_{30}$	0	0	0	0

$M_s$  and coercivity  $H_c$  for various MnAl films after annealing at 410 °C for 30 min and the substrate temperature  $T_s=30$  and 100 °C. The maximum  $M_s$  of about 420 emu/cc and a maximum  $H_c$  of about 3000 Oe was obtained for the  $\text{Mn}_{50}\text{Al}_{50}$  sample with  $T_s=30$  °C. In general, the  $\epsilon \rightarrow \tau$  phase transformation occurred during the annealing treatment. Since the  $M_s$  of the annealed films decreased with increasing  $T_s$ , the transformation fraction should decrease with increasing  $T_s$ , i.e., the films deposited at lower  $T_s$  have a large and more perfect crystalline structure than the films deposited at higher  $T_s$ . In other words, at a low substrate temperature the sputtered atoms arriving on the substrate should not have enough energy to form the metastable  $\tau$  phase or the equilibrium  $\beta$  and  $\gamma$  phases, and the  $\epsilon$  phase was formed due to the superquenching effect.

Figure 2 shows the stress-temperature curve of the  $\text{Mn}_{50}\text{Al}_{50}$  film during the whole annealing process, which were recorded at a heating rate of 5 °C/min from room temperature to 450 °C and then furnace cooled to room temperature. We observed a compression stress for the heating run roughly below 220 °C, and a tension stress roughly above 220 °C during the cooling run. This suggests that the structure phase transformation from  $\epsilon$  to  $\epsilon'$  phase happens roughly below 220 °C and then it transforms to  $\tau$  phase

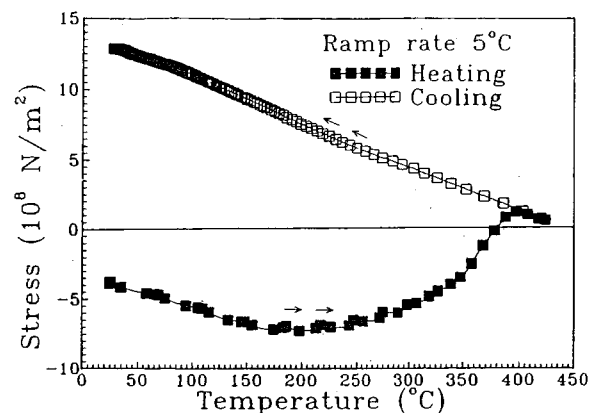


FIG. 2. The stress of the  $\text{Mn}_{50}\text{Al}_{50}$  film as a function of temperature between room temperature and 450 °C (closed square: heating run; open square: cooling run).

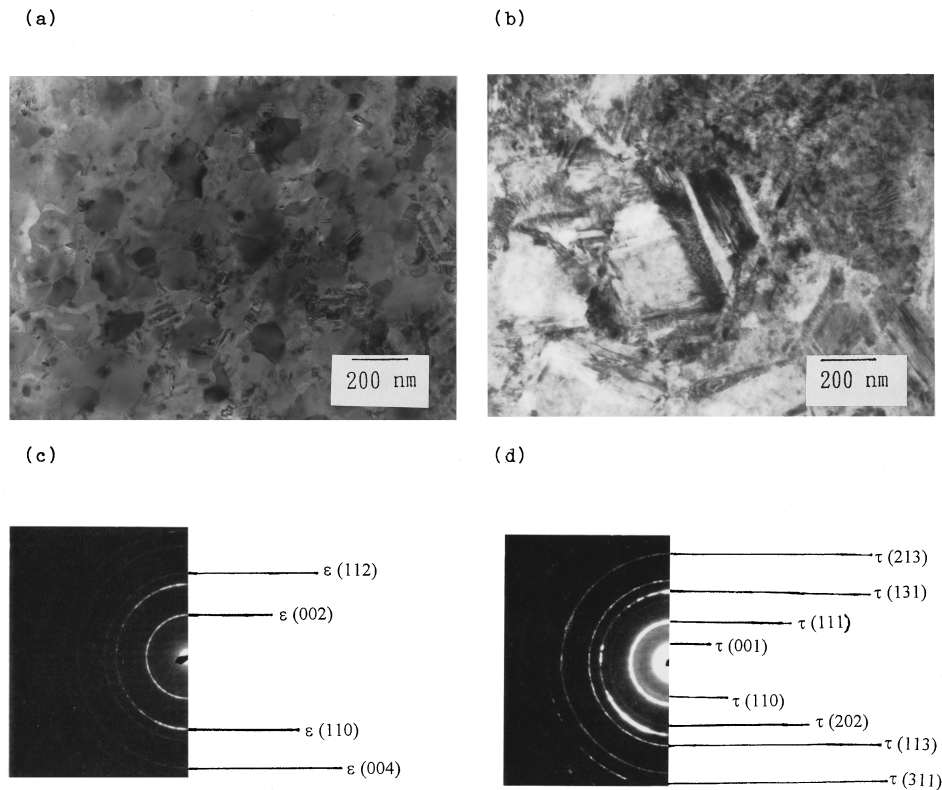


FIG. 3. (a) Transmission electron bright field images of the as-deposited  $\text{Mn}_{50}\text{Al}_{50}$  samples with  $T_s=30^\circ\text{C}$ . (b) Transmission electron bright field images of the  $\text{Mn}_{50}\text{Al}_{50}$  samples with  $T_s=30^\circ\text{C}$  and annealing at  $410^\circ\text{C}$  for 30 min. (c) Transmission electron diffraction patterns of the as-deposited  $\text{Mn}_{50}\text{Al}_{50}$  samples with  $T_s=30^\circ\text{C}$ . (d) Transmission electron diffraction patterns of the  $\text{Mn}_{50}\text{Al}_{50}$  samples with  $T_s=30^\circ\text{C}$  and annealing at  $410^\circ\text{C}$  for 30 min.

roughly between  $220$  and  $450^\circ\text{C}$ . After cooling to room temperature, the residual stress  $\sigma$  of this  $\tau$ -phase film is about  $13 \times 10^8 \text{ N/m}^2$ . Therefore, the high coercivity is explained due to the high magnetocrystalline anisotropy constant  $K_1$  of the  $\tau$  phase ( $K_1 \cong 10^7 \text{ erg/cm}^3$ )<sup>1</sup> and the magnetoelastic energy  $E_{\text{me}}$  (Ref. 11) arises from the residual stress ( $E_{\text{me}} \propto \sigma = 13 \times 10^8 \text{ N/m}^2$ ) of MnAl films after the shear transformation.

The microstructure grain sizes and the phases of the samples were studied by transmission electron microscopy. Figure 3 shows the transmission electron bright field images and diffraction patterns of the as-deposited  $\text{Mn}_{50}\text{Al}_{50}$  samples with  $T_s=30^\circ\text{C}$  [Figs. 3(a) and 3(c)], and the  $\text{Mn}_{50}\text{Al}_{50}$  samples with  $T_s=30^\circ\text{C}$  and annealing at  $410^\circ\text{C}$  for 30 min [Figs. 3(b) and 3(d)]. It is clear that the nonmagnetic  $\epsilon$  phase as shown in Fig. 3(c) with a grain size of roughly  $100 \text{ nm}$  as shown in Fig. 3(a) for the as-deposited samples transforms into a metastable ferromagnetic  $\tau$  phase as shown in Fig. 3(d) with a platelike grain size of roughly  $300 \text{ nm}$  as shown in Fig. 3(b).

In conclusion, we observed that during annealing at  $410^\circ\text{C}$ , the nonmagnetic  $\epsilon$  phase with a grain size of roughly  $100 \text{ nm}$  transforms into a metastable ferromagnetic  $\tau$  phase with a platelike grain size of roughly  $300 \text{ nm}$ . The structure phase transformation from  $\epsilon$  to  $\tau$  phases were related to the variation of the stress from compression to tension. The high coercivity can be explained by the high magnetocrystalline

anisotropy constant of the  $\tau$  phase, and the magnetoelastic energy arises from the residual stress of Mn–Al films after the shear transformation.

## ACKNOWLEDGMENT

The authors are grateful for financial support by the National Science Council of the ROC under Grant Nos. NSC86-2112-M-001-014 and NSC85-2216-E-002-017.

<sup>1</sup>H. Kono, J. Phys. Soc. Jpn. **13**, 1444 (1958).

<sup>2</sup>Y. Z. Vintaykin, V. A. Udovenko, I. S. Belyatskaya, N. N. Luarsabishvili, and S. Y. Makushev, Fiz. Met. Metalloved. **38**, 398 (1974).

<sup>3</sup>J. Van Landuyt, G. Van Tendeloo, J. J. Van Den Broek, and H. Donkersloot, J. Magn. Magn. Mater. **15**, 1451 (1980).

<sup>4</sup>P. C. Kuo, Y. D. Yao, J. H. Huang, and C. H. Chen, J. Magn. Magn. Mater. **115**, 183 (1992).

<sup>5</sup>J. H. Huang and P. C. Kuo, Mater. Sci. Eng. B **22**, 256 (1994).

<sup>6</sup>A. Morisako, M. Matsumoto, and M. Naoe, IEEE Trans. Magn. **23**, 2470 (1987).

<sup>7</sup>A. Morisako, M. Matsumoto, and M. Naoe, J. Appl. Phys. **61**, 4281 (1987).

<sup>8</sup>J. X. Shen, R. D. Kirby, and D. J. Sellmyer, J. Appl. Phys. **67**, 4929 (1990).

<sup>9</sup>A. Morisako, N. Kohshiro, M. Matsumoto, and M. Naoe, J. Appl. Phys. **67**, 5655 (1990).

<sup>10</sup>M. Matsumoto, A. Morisako, and J. Ohshima, J. Appl. Phys. **69**, 5172 (1991).

<sup>11</sup>B. D. Cullity, *Introduction to Magnetic Materials* (Addison-Wesley, London, 1972), p. 270.